Microscopic effects at GaAs/Ge(100) molecular-beam-epitaxy interfaces: Synchrotron-radiation photoemission study

A. D. Katnani, P. Chiaradia,* H. W. Sang, Jr., P. Zurcher,† and R. S. Bauer
Xerox Palo Alto Research Center, 3333 Coyote Hill Road, Palo Alto, California 94304
(Received 30 July 1984)

We have measured the evolution of abrupt GaAs/Ge(100) interfaces to study the relationship between the valence-band discontinuity (ΔE_v) and growth properties on an atomic scale. We used soft x-ray photoemission, low-energy electron diffraction, and Auger electron spectroscopy. The interface was obtained by evaporating Ge (at $< 10^{-9}$ Torr and intentionally coevaporating at an overpressure of As_4) *in situ* onto a molecular-beam-epitaxy- (MBE-) grown GaAs sample under epitaxial growth conditions. The MBE-grown GaAs(100) provided different surface reconstructions with controllable starting anion-to-cation ratio. We present a new core-intensity-analysis method for determining thin-film growth independent of the adlayer thickness calibration. For all interfaces, a monolayer of segregated As was observed at the free Ge surface. This suggests that the As-stabilized Ge surface phase formation plays an important role in determining the interface growth. The value we obtain for ΔE_v is (0.47±0.05) eV, independent of both the initial clean GaAs(100) surface properties and the evolution of the Fermi level. We propose that the driving force for MBE interface formation always yields a unique, low-energy equilibrium structure at the materials transition region, although its extent may vary by as much as a couple of atomic layers. However, the observed constancy of ΔE_v suggests that the contribution of any perturbation caused by variations in the local microscopic properties of the interface (e.g., dipoles) is very small compared to the intrinsic (perhaps bulk) mechanism that determines ΔE_v.

I. INTRODUCTION

Semiconductor heterojunction interfaces have stimulated many experimental and theoretical studies over the past two decades.[1–34] One of the main thrusts of such studies is the band lineup at the interface, i.e., the distribution of the band-gap difference between the valence band, ΔE_v, and the conduction band, ΔE_c. From a theoretical point of view, fully-self-consistent calculations[5–7] encounter great difficulties in dealing with the band lineup at a realistic interface. Therefore, simple models are used to calculate ΔE_v.[9–13] There is experimental evidence that the widely used Anderson surface electron affinity rule[9] provides incorrect values for the band offset.[14] Some of the other models are based solely on using bulk parameters and completely ignore properties of the surfaces or interface.[12,13] Systematic experimental studies of a large number of heterojunctions consisting of group-III-V and and II-VI semiconductors with Ge or Si have been performed to test the validity of such an approximation.[15–18] The results of this study are then compared with theoretical predictions.[18] A general accuracy limit on the order of ± 0.10 eV is estimated from such a comparison. Furthermore, this general accuracy limit defines an overall estimate of the contribution of the local microscopic effects to ΔE_v, i.e., interface dipoles.[35]

Other experimental studies have been performed on prototypical interfaces between semiconductors that are lattice-matched, simple to prepare, and theoretically well understood.[19–30] Among such interfaces is the GaAs/Ge interface, which has been extensively studied by a number of authors.[19–30] However, all available experimental results on ΔE_v for this interface show a consistency within ~ 0.3 eV. It is important to understand the various factors that cause such a spread in the measured ΔE_v's. Is this spread due to variation in the local microscopic properties of the interface (morphology of the overlayer, variation in the atomic arrangement at the starting surface, surface orientation, etc.) or to different methodologies (preparation procedure, analysis, etc.) used by different authors? The questions reduce to whether the scattering of ΔE_v can be correlated with some chemical or structural parameter that can be experimentally controlled.

We have performed a systematic study of a large number of GaAs/Ge(100) interfaces to address the above issues. Changes in the local microscopic effects are induced by varying the GaAs(100) surface reconstruction and, thereby, the surface stoichiometry. For some of the interfaces, As_4 has been introduced during the deposition of the overlayer. By following the same preparation procedure under the same conditions and using the same data analysis for all the interfaces we studied, we minimize the contribution to ΔE_v due to the methodology. Therefore, our study focuses on the variations in the interface properties and their effects on ΔE_v.

We have studied the initial stages of interface formation. The evolution of the As($3d$) line shape shows that the As species is involved in a series of chemical processes at the interface and 1 ML (ML denotes monolayer) of As is segregated at the surface of a thick Ge overlayer, while the Ga($3d$) line shape shows that if Ga does have any strong chemical activity it is confined to the interfacial region. This stationary position of the cation is used as a novel method for analyzing the evolution of the different

 ©1985 The American Physical Society

atomic constituents during the heterojunction growth, independent of the Ge-overlayer thickness.

The measured ΔE_v is the same for all the different starting surfaces we have investigated, regardless of the Fermi-level position in the gaps, within an experimental uncertainty of ± 0.05 eV. The different kinds of chemical and structural variations induced at the intimate GaAs/Ge(100) interface do *not* contribute to ΔE_v by more than ± 0.05 eV. Such a result explains the success of the purely bulk semiconductor model for heterojunction band offsets.[12,13]

II. EXPERIMENT

Several surface-sensitive experimental techniques [soft-x-ray photoelectron spectroscopy (SXPS), low-energy electron-diffraction (LEED), and Auger-electron spectroscopy (AES)] were used to probe clean GaAs(100) surfaces and Ge overlayers. Photons emitted from SPEAR at the Stanford Synchrotron Radiation Laboratory (SSRL) were monochromatized using a grasshopper monochromator. Photoelectrons emitted from the valence band and from the As(3*d*), Ga(3*d*), and Ge(3*d*) core levels were collected using a standard PHI double-pass cylindrical mirror analyzer.

Si-doped GaAs(100) wafers (5×5 mm) were chemically polished and etched in $5H_2SO_4$:$1H_2O$:$1H_2O_2$ solution. The wafers were mounted on molybdenum holders with In contacts. Auger spectra of an untreated wafer showed C and O as the major contaminants. For some wafers it was possible to remove the O contamination by annealing only. However, it was necessary to use ion bombardment to sputter-off C contaminations. Usually, after sputtering for 30—40 min the Auger signal of O and C is reduced to below the detectability limit of AES. The sample was annealed at 540 °C for 30 min after sputtering. The LEED pattern from a sputtered-annealed sample showed a 1×1 or 4×6 (or any of its derivatives) ordering of the surface layer. The Ga- and As-source temperatures were kept at 950 and 280 °C, respectively. The sample temperature was kept at 535 °C. These settings gave an As_4/Ga ratio of greater than 3 and a growth rate of ~ 100 Å/min. The different GaAs(100) surface reconstructions were prepared by controlling the As_4 flux and the substrate temperature soon after growing a thick buffer layer.[28–30] The Ge overlayer was grown epitaxially on the surface at a substrate temperature of 320 °C. Under this condition, one obtains the most abrupt interface possible.[23,24] The pressure was $(7–9)\times10^{-10}$ or $(7–9)\times10^{-7}$ Torr of As_4 during the growth of the Ge overlayer.

The Fermi level of the spectrometer was determined from the Fermi edge of a thick film of Au. Changes in the Fermi-level position in the gaps were monitored by the shift in the Ga(3*d*) and Ge(3*d*) peak positions with Ge coverage. The valence-band discontinuity was estimated from the distance in energy between the valence-band edges of the clean surface and Ge overlayer after subtracting the change in band bending. This method yielded consistent results with the method described in Ref. 20. The overall experimental resolution was 0.15—0.4 eV. The observed experimental reproducibility between different data sets taken over a three year period was ± 0.05 eV.

The GaAs(100) surface was chosen because of the large variety of surface reconstructions and stoichiometries available. Furthermore, the differences among these surface structures and anion-to-cation ratios serve as a typical example of the variations one would expect to influence the band offsets, as we will discuss later. The differences among these surface reconstructions test the effect of the local microscopic properties of the interface on the band offsets.

The GaAs(100) surface exhibits a number of reconstructions, among them 4×6, $c(8\times2)$, $c(2\times8)$, and $c(4\times4)$. The surface stoichiometry as derived from our core-level photoemission measurements[36] and from measurements of other authors[30–34] correlates with the surface ordering. The measured As/Ga ratio increases as the surface ordering changes from 4×6 to $c(8\times2)$ to $c(2\times8)$ to $c(4\times4)$ (as shown in the inset of Fig. 12). While the exact surface-As concentration is the subject of much recent controversy,[30–34] this ordering provides an unambiguous identification for our heterojunction study.

III. 3*d* CORE-LEVEL PHOTOEMISSION

As(3*d*), Ge(3*d*), and Ga(3*d*) spectra have been recorded for the clean surface and at increasing Ge coverages for all the interfaces we studied. Figure 1 shows a typical sequence of these core levels taken for the clean GaAs(100) $c(8\times2)$ surface and for consecutive coverages of Ge.

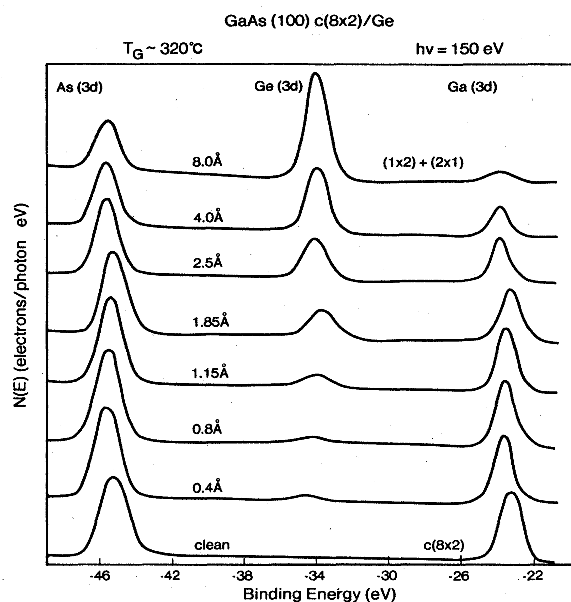

FIG. 1. Evolution of the core-level photoemission from As(3*d*), Ge(3*d*), and Ga(3*d*) at $h\nu=150$ eV for GaAs(100) $c(8\times2)$ and increasing coverage of epitaxial Ge overlayers. Spectra taken at different Ge coverages are shown. The substrate temperature was set at 320 °C during the growth. The LEED pattern for the surfaces corresponding to the first and last spectrum are reported.

A. Core-level line shape

1. As(3d)

The upper half of Fig. 2 shows the As($3d$) line shape for the $c(2\times8)$, $c(4\times4)$, and 4×6 surfaces at $h\nu=106$ eV. Surface and bulk components have been deconvoluted using a Gaussian fit and assuming that the spin-orbit splitting and branching ratio are the same for all components.[37] The shaded doublet corresponds to the contribution of the As atoms in bulk GaAs for each surface. We identify the shifted peaks with the rearranged surface-As atoms. The $c(4\times4)$ surface exhibits an extra doublet which we attribute to the formation of an As—As bond.[38] Note that the bonding and intensity of these shifted peaks are *different* for the different surfaces. This observation demonstrates the distinct bonding and stoichiometry variations among the GaAs(100) surface reconstructions.

Because of the complexity of the problem we did not attempt to apply the above fitting routine to the As($3d$) line shape after the deposition of Ge. However, we observed that the As($3d$) linewidth *decreases* with increasing Ge coverage. Eventually, it saturates and does not change even with very thick Ge overlayers. Because we still observe a signal from As($3d$) in the absence of a significant Ga($3d$) signal at very high Ge coverages (160 Å), As must be segregated to the top of the Ge layer. The lower half of Fig. 2 shows the final As($3d$) line shape observed even at thick Ge coverage. From the intensity of this As($3d$) signal we estimate that at least 1 ML of As caps the Ge layer regardless of the starting GaAs(100) surface-As concentration.[28,29] The reduced As($3d$) linewidth suggests a more localized anion bonding at the Ge:As surface than in GaAs. This is consistent with the formation of As lone pairs, as seen in GeAs.[39] The evolution of the different As($3d$) line shapes to a unique one at thick Ge coverage suggests that the chemistry of the interface should either be different for the different starting surfaces or distributed over differing effective interface widths.

2. Ga(3d)

Figure 3 shows the Ga($3d$) line shape for the three surface reconstructions we studied. The spin-orbit splitting, 0.45 eV, and the branching ratio, 0.65, were obtained from bulk-like Ga($3d$) line shape.[37,40] The figure emphasizes the differences among the three surface reconstructions. Notice that the surface contribution to the line shape is very small, except for the 4×6 surface. The evolution of the Ga($3d$) line shape does *not* indicate strong chemical activity of the Ga atoms up to 7 Å of Ge coverage. The slight changes in line shape we observed above 7 Å can be related solely to the out-diffusion of a small amount ($<5\%$ of a monolayer) of Ga. The peak-position shift indicates a smooth decrease in the binding energy that satu-

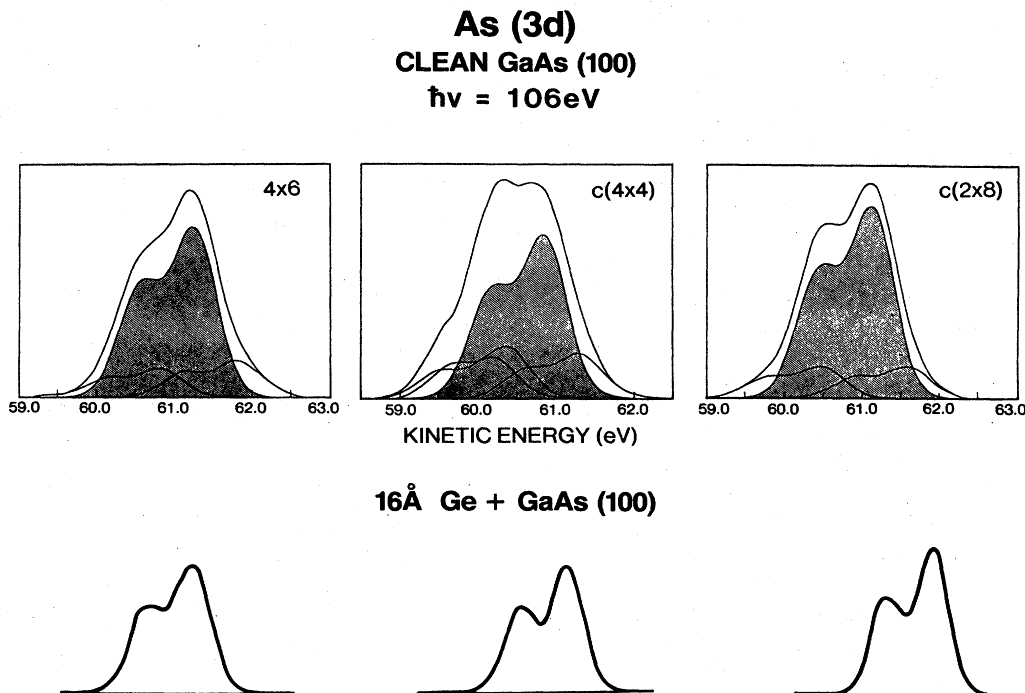

FIG. 2. As($3d$) line shape for GaAs/Ge(100) at $h\nu=106$ eV for the clean and thickly covered Ge 4×6, $c(2\times8)$, and $c(4\times4)$ surfaces. The bulk-related component is indicated by the shaded area. The energy positions and intensities of the surface components for each line shape are different, demonstrating the differences among the three surface reconstructions. The $c(4\times4)$ exhibits an extra doublet which is associated with a quarter-monolayer of an amorphous As overlayer. The initial and final As($3d$) line shapes are shown because of the difficulties involved in fitting the line shape at intermediate coverages. The final As($3d$) line shape is the same in intensity and width for all starting surfaces studied here.

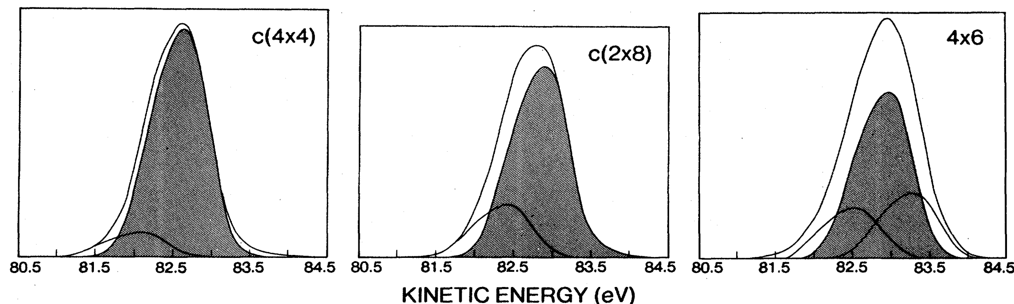

FIG. 3. Ga(3d) line shape taken with 106 eV photon energy for three surface reconstructions of GaAs(100). The shaded area again identifies the bulk contribution to the line shape. This figure emphasizes the distinct differences between the three surface reconstructions. The evolution of the line shape with increasing Ge coverage shows an exponential attenuation of the peak intensity and a smooth shift in the energy position for all interfaces studied here.

rates at 4 Å of Ge coverage.[24] Several authors have observed that the cation peak position and the valence-band edge shift by the same amount when metals or oxides are deposited on GaAs.[41,42] Therefore, we attribute the observed shift in Ga(3d) to changes in band bending rather than any metallic clustering.

3. *Ge(3d)*

The initial Ge(3d) line shape is broad, as expected, because of the different bonding configurations of Ge adatoms at small coverages. As the Ge coverage reaches 1 ML, the linewidth decreases, indicative of an epitaxial accommodation to the substrate lattice. The decrease in linewidth with coverage also indicates that the chemically reacted Ge is localized at the interface. The final Ge(3d) line shape is broader than that expected from pure Ge because of the presence of the capping As monolayer discussed above. Because of the complexity of the early stages of interface formation, we did not attempt to use our fitting routine to deconvolute the Ge(3d) line shape. Misleading information can easily be obtained from such a technique under the present circumstances.

B. Core-level peak intensity

1. *Normalized intensity versus Ge coverage*

Figure 4 shows the attenuation of the core-level emission with Ge coverage for both As and Ga in the case of the 4×6 surface. The intensities are the individual core-level emission peak areas normalized to the sum of the peak areas after linear background subtraction. A quadratic background does not significantly affect the results. We have neglected the small differences in cross section and escape depth among As, Ge, and Ga in the energy range of our spectra. We estimate the correction to be less than 10%.[23,24] Figure 4 shows that, after deposition of the first half-monolayer of Ge (0.7 Å) onto a 4×6 surface, the As-peak intensity has grown instead of being attenuated. In agreement with this observation, the decrease of the Ga-peak intensity is initially faster than expected from escape-depth considerations. After this initial "abnormal" trend, the Ga-peak intensity decreases exponentially with an escape depth of 4.5 Å, in agreement with existing data in the literature.[43] No detectable Ga out-diffusion occurs up to a Ge coverage of about 6 ML,

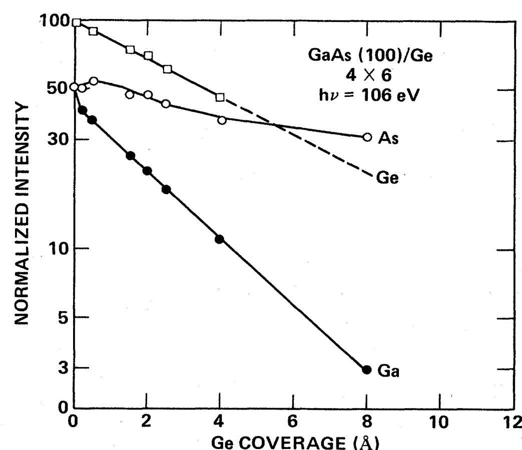

FIG. 4. Logarithmic plot of the relative intensities (i.e., peak intensity normalized to the sum of the 3d core-level areas) of As(3d), Ge(3d), and Ga(3d) as a function of increasing Ge coverage on the GaAs(100) 4×6 surface. The core levels were taken with 106 eV photon energy. Note that the Ga(3d) relative intensities follow an exponential attenuation with an attenuation length of 5 Å, while the As(3d) relative intensity initially decreases and then saturates at Ge coverages above 6 Å. This indicates no measurable out-diffusion of Ga and the segregation of As to the free Ge surface.

unlike that reported by other authors.[24] Instead, Fig. 4 clearly shows that As segregates at the surface.

2. Stationary-cation analysis: Intensity-versus-intensity plots

To gain further insight into the evolution of the As and Ga core levels with coverage, we have devised a new method of analysis in which we plot the normalized intensity of one component (As or Ge) versus another (Ga). This scheme is based on the fact that Ge, As, and Ga atoms have approximately the same cross section, and that the escape depth of photoelectrons across the Ge layer is the same as that of the GaAs and its constituents. Therefore, the total intensity (which is proportional to the number of atoms within the attenuation length of photoelectrons) is the same, *independent* of the Ge coverage. Hence, such a methodology allows one to directly observe the evolution of the core-level signals without calibrating the overlayer thickness. Errors due to coverage uncertainties are avoided. The curves obtained from such analysis are usable only when one substrate constituent is recognized to be *stationary* (i.e., not out-diffusing). Metal[44,45] and oxide[41] overlayers have previously been shown to usually leave the semiconductor cation unmoved (i.e., attenuates exponentially with increasing overlayer coverage). In the epitaxial abrupt growth regime for Ge on GaAs, this is usually the case for the Ga, as shown in Fig. 4.

Examples of this new methodology are given in Fig. 5, where such a plot (hereafter called an intensity-versus-intensity plot, abbreviated as *I-I* plot for simplicity) is shown for the 4×6, $c(8\times2)$, and $c(4\times4)$ surfaces, respectively. The "ideal" case (dashed line) occurs if no exchange reaction or interdiffusion takes place. Both As and Ge curves differ considerably from such an abrupt, unmixed ideal interface situation. In the *I-I* plot of Fig. 5, the Ge-coverage increase corresponds to changes along the curves, as pointed out by the arrows. The As curve is always above the ideal line. This indicates an As outdiffusion through the Ge overlayer independent of starting surface stoichiometry. Moreover, all As curves extrapolate to the *same* amount of As [$(27\pm2)\%$], *independent* of the starting surface As concentration.

Distinct differences occur at the onset of the As curves in the three cases reported in Fig. 5. For the 4×6 surface the As curve immediately starts moving upwards, indicating that As is driven to the surface, most probably from the underlying GaAs layers. A simple picture in which Ge atoms first bond to surface Ga, leaving As atoms unburied, would lead to a horizontal onset of the As curve, contrary to the experimental finding. On the other hand, the $c(4\times4)$ surface has a completely different behavior as far as the onset of the As-curve behavior is concerned. Independent of the starting point being different (i.e., higher As signal for this surface compared to the 4×6), the As curve initially drops and runs close to the ideal case. This points out that Ge simply covers the As-saturated $c(4\times4)$ surface without any major rearrange-

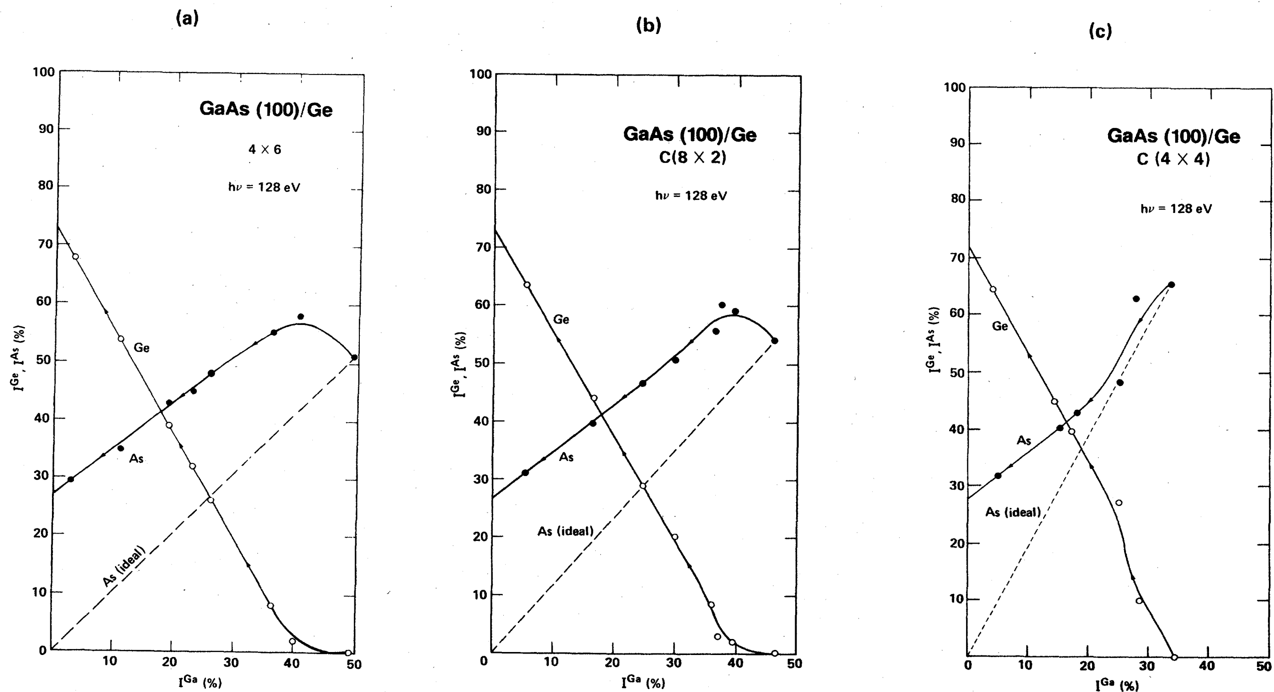

FIG. 5. Stationary cation analysis: The facts that Ga atoms are stationary and Ga, As, and Ge have the same atomic cross section and escape depth in the energy range of concern led us to devise a novel method to monitor the interface formation without necessarily knowing the thickness of the overlayer. As shown in the figure, the As($3d$) and Ge($3d$) relative intensities are plotted as a function of the Ga($3d$) relative intensity. The core-level spectra were obtained with 128 eV photon energy. The figure demonstrates the application of this method for the GaAs(100) 4×6, $c(8\times2)$, and $c(4\times4)$ interfaces with Ge. The onset of the As curve for the three surfaces is different; however, the final relative intensity of As($3d$) is the same.

ment at the initial coverage stage. Then at higher Ge coverage (above ~1 ML), an exchange reaction between Ge and As takes place and As floats at the surface.[26–29] The case of the $c(8\times2)$ surface is an intermediate one, as one would expect if surface chemical processes *scale* with the initial As/Ga ratio. Indeed, the case of the $c(8\times2)$ surface is very analogous to that of 4×6. This suggests that the difference in surface atomic structure (primitive versus centered) is less important to interface formation than surface chemistry (stoichiometry).

All three cases extrapolate to the same endpoint, $(27\pm2)\%$, regardless of the starting point. This demonstrates that the As-stabilized Ge-surface phase formation influences the interface growth. The LEED pattern of this Ge:As surface reconstruction on GaAs/Ge(100) consists of two 2×1 domains and is reproducible.[46] The pattern is the same for all starting GaAs(100) surfaces and it does not change even upon deposition of a thick (>2000 Å) Ge layer. Furthermore, experimental studies associated this LEED pattern with the formation of a $GeAs_x$ compound.[27,39] This commoness of primitive and centered starting structures again suggests that surface stoichiometry is a greater determinant of interface-formation behavior than the initial surface-bonding structure.

The observation of the As capping layer of the Ge surface for all the interfaces we studied raised a question about the origin of this layer. Recently, Neave *et al.* suggested contamination from the environment as the origin of this layer.[32] However, Monch and Gant observed at least 1 ML of As at the free Ge surface of a GaAs/Ge(110) interface, where the GaAs surfaces was prepared by cleavage and with no As source in the experimental chamber.[23] The ambient probably does not contribute significant As because a sputtered-clean Ge surface did not show any As contamination even after being left in our experimental chamber for hours. Furthermore, we did not observe any As on the surface of a Ge buffer layer when grown on a pure-Ge substrate. These observations suggest that As keeps *floating* at the free surface during the Ge deposition on GaAs, and that indeed As is present due to segregation rather than environmental contamination. In fact, total-energy calculations show that As segregates to the Ge free surface for the system to attain its minimum energy.[47]

IV. FERMI LEVEL AND BAND OFFSETS

The observed core-level-energy and line-shape difference among the various initial surfaces used in our study, together with their evolution during interface formation, serve as "fingerprints" of the changes induced at the interface. In this section we will discuss the influence of these changes on the charge redistribution and/or the band lineup at the interface. These changes are inferred from the evolution of the Fermi-level position in the gaps on both sides of the interface with increasing Ge coverage.

A. Core-level and valence-band-edge energies

The Ga(3*d*) and Ge(3*d*) peak positions are obtained from center of gravity of the core-level line shape (i.e., the midpoint of the linewidth at half the peak height, full width at half maximum). Because Ga is not involved in strong chemical activity and the surface contribution to the Ga(3*d*) line shape is small, as we discussed earlier, the relative shift of the center of gravity and that of the position of $3d_{5/2}$ with increasing Ge coverage are the same. The regime where the Ge(3*d*) line shape is broad is not important for our measurement. Although, at coverages above 4 Å (where the Ge band structure is fully developed), the Ge(3*d*) line shape is broader than expected, the distance in energy between the Ge valence-band edge and the Ge(3*d*) center of gravity is the same as obtained from other authors' work.[39] Therefore, in that regime we considered the center of gravity as representative of the peak energy position.

Figure 6 shows a typical evolution of the GaAs valence-band angle-integrated photoemission at $h\nu=130$ eV as a function of Ge coverage for the $c(8\times2)$ surface. The arrows point out those features of the clean spectrum undergoing the most prominent changes. It is clear that the Ge valence-band spectral features (e.g., disappearance of heteropolar gap) are fully developed at Ge coverages between 4 and 8 Å, in agreement with theoretical predictions[48] and similar to that observed for GaAs/Ge(110) interfaces.[29]

The energy position of the valence-band maximum is determined from the linear extrapolation of the valence-band edge. The results of this method were checked against the results of the more precise method developed by Kraut *et al.*[20] We found an agreement within 0.1 eV. Because we are interested in relative distances and not in the absolute position of the valence-band maximum, such error cancels out.

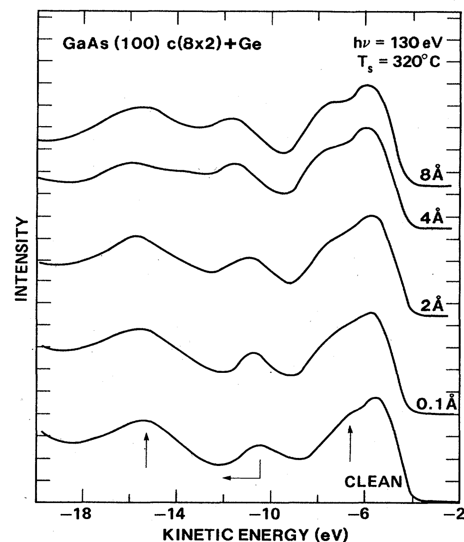

FIG. 6. Evolution of the valence-band spectral features with increasing Ge coverage for the GaAs(100) $c(8\times2)$ surface taken with 130 eV photon energy. The most relevant differences between the GaAs and Ge spectral features are pointed out in the figure. Note that at coverages above 4 Å all electronic structural features of the valence band of Ge are fully developed.

B. Fermi level

The position of the Fermi level (E_F) with respect to the top of the valence band on each side of the interface can be experimentally determined by measuring the energy position of a core level relative to the Fermi edge of the analyzer (measured from an *in situ* metal deposition during the same experiment). The binding energy of the core levels are taken from the work of Kraut *et al.*[39] Figure 7 shows the relative position of E_F and the top of the valence band for both the GaAs substrate and the Ge overlayer as a function of the Ge coverage, in the case of a $c(4\times4)$ surface. The starting GaAs MBE-grown buffer layer appears to be intrinsic (E_F at midgap). The final E_F position in Ge corresponds to an almost degenerate n-type material. Figure 8 shows a comparison of the evolution of the Fermi-level position with respect to the valence-band edges in GaAs and Ge for different initial reconstructions, namely 4×6, $c(8\times2)$, and $c(4\times4)$, in order of increasing surface As concentration, respectively. Note that there is no unique position of the Fermi level in the GaAs(100) band gap, such as a pinning of E_F by defect states at the GaAs(110) surface.[49,50] The condition imposed on energy levels on both sides of the interface to create a dipole layer are too severe to reasonably expect such a Fermi-level stabilization.[35] Moreover, both the initial and final positions of E_F with respect to the GaAs valence band are correlated with the As/Ga ratio of the initial reconstruction.[36,49]

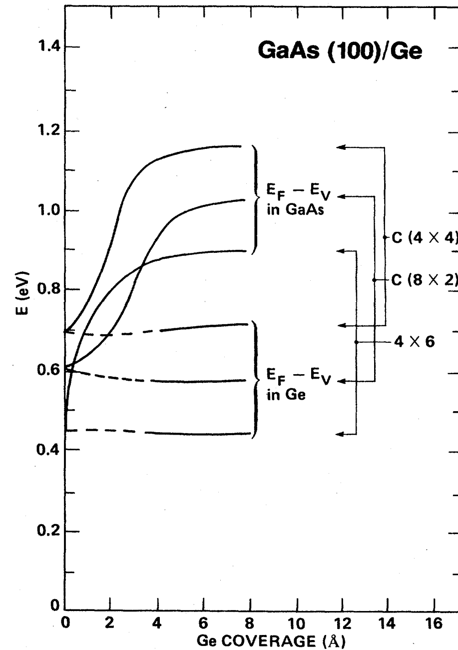

FIG. 8. Evolution of the Fermi-level position with respect to the valence-band edges of Ge and GaAs during interface formation between GaAs(100) and Ge. The figure shows a comparison among the distant starting surfaces of GaAs(100). Again, the difference between the curves related to the same interface defines the band offset at that interface.

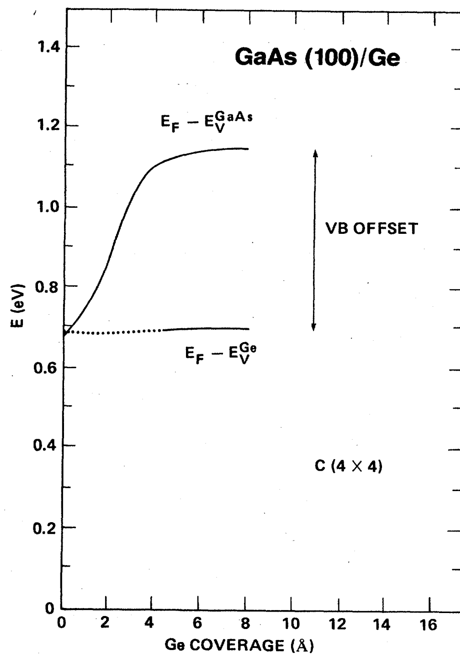

FIG. 7. Evolution of the Fermi-level position with respect to the valence-band edges of Ge and GaAs during interface formation between GaAs(100) $c(4\times4)$ and Ge. The difference between the two curves defines the band offsets above a Ge coverage of 6 Å. At the early stages the difference is meaningless because the electronic structure of the valence band of Ge is not yet fully developed.

C. Band-gap discontinuities

We have measured ΔE_v for the heterojunctions at issue by applying a method based on the determination of the valence-band edge.[18] Figure 9 shows a plot of the differ-

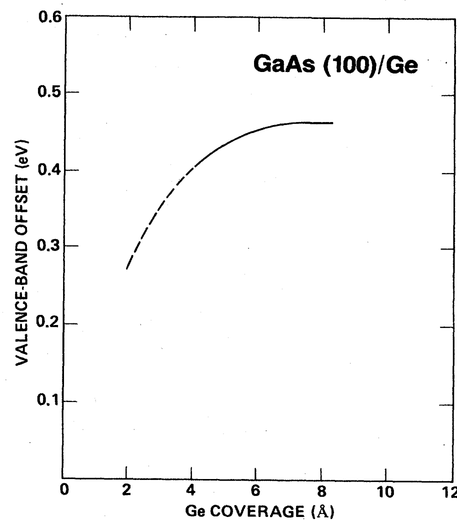

FIG. 9. Typical behavior of the valence-band offset for a GaAs/Ge(100) heterojunction as a function of Ge coverage. The dashed line represents the region of coverage in which the electronic structure of the valence-band edge of Ge is not fully developed.

ence between the shift in the valence-band edge and the Ga(3d) line shape as a function of Ge coverage. Below a certain coverage, the valence-band structure of the overlayer is not fully developed. Clearly, at small coverages this difference should be zero because the shift in both the valence-band edge and Ga(3d) line shape is due mainly to the change in band bending. The dashed line indicates the coverage region where the shift in the valence-band edge is composed of two components. One is due to the change in band bending and the other is due to development of the Ge-overlayer electron structure. Note that the difference is practically constant in the range 6—8 Å (4—6 ML). At this stage the difference is fully indicative of ΔE_v alone.

The measured ΔE_v is the same [(0.47±0.05) eV] *regardless* of all the variations induced at the interface as presented in Sec. III. Previously reported experimental values referring to the same GaAs/Ge(100) interface ranged from (0.40±0.1) eV, for an MBE-grown $c(2\times8)$ surface,[30] to 0.55 and 0.66 eV for Ga- and As-rich initial surfaces, respectively, cleaned by sputter annealing.[22] Our method of valence-band-edge analysis is the same as in Ref. 18. It is worthwhile to note that, by using the alternative method based on core-level-energy differences across the interface,[20] we find values for the ΔE_v that are systematically larger by ~0.08 eV. Possible reasons for this small discrepancy have already been discussed in the literature.[30]

We do *not* observe any correlation between ΔE_v and the initial As/Ga ratio, or whether the substrate surface had a primitive (i.e., 4×6) or centered [i.e., $c(4\times4)$, $c(2\times8)$, or $c(8\times2)$]. We must consider how this relates to chemical composition and ordering at the final heterojunction interface. In this context, by interface we mean the transition region between the first complete Ge plane and the first complete plane of As or Ga. For an epitaxial heterojunction, this region extends over a few atomic planes.[51,52] In principle, two hypotheses can be formulated: (1) either the ΔE_v is the same *because* the microscopic properties of the heterojunction are the same, or (2) it is the same *despite* the fact that the microscopic properties are different. At the present time this question cannot be convincingly answered experimentally because extensive modeling of core-level line shape, even when it is possible, does not yield a unique description of the atomic arrangement. However, the *evolution* of the interface growth suggests that the heterojunction interface might actually be different, on an atomic scale, among the number of samples covering the different surface reconstructions of GaAs(100), where we measured the *same* ΔE_v. In fact, just accounting for the As monolayer at the free Ge surface suggests that the evolution goes in the direction of enriching the interface with As when the starting GaAs(100) surface is As depleted. The amount, ordering, and chemical bonding of the segregated As, as well as the evolution of the As(3d) line shape, tend to emphasize the irrelevance of the chemistry and stoichiometry of the starting surface. In turn, we propose that the driving force for MBE interface formation always yields a unique, low-energy equilibrium structure at the material's transition region, although its atomic extent may vary by as much as a couple of atomic layers. Therefore, if there is any "nanoscopic" dipole contribution to the valence-band discontinuity, it appears to be either very small or the same (within ±0.05 eV).

V. As_4CO-EVAPORATION DURING INTERFACE FORMATION

The segregation of As on the free Ge(100) surface and the correlation between the starting As-surface coverage and the final E_F in the gaps raise a question about the role of As in interface formation. The facts that As is not supplied by the environment (as we discussed earlier) and that we observe the same amount of As regardless of the starting As coverage require that the As out-diffuse from the bulk GaAs or be supplied by anion clusters in the near-surface region. One observation consistent with this is the report of Joyce and Foxon[53] of GaAs-surface enrichment upon annealing MBE films grown with As_4. The depth from which such As is supplied is not clear; nevertheless, it probably will increase the width of the interface if it is supplied from the first few monolayers of GaAs. If As is intentionally supplied to the interface during Ge epitaxial growth, would ΔE_v and/or E_F be affected?

To answer the above question we performed a series of experiments in which we introduced an overpressure of As_4 during the MBE deposition of Ge. The results of these experiments point out that the presence of As in the environment during the Ge evaporation modifies a number of parameters in the initial stages of interface formation.

A. Core-level intensity

The core-level intensities clearly show an As uptake at submonolayer coverages. In Fig. 10 the As(3d) core-level signal is reported as a function of the Ga(3d) intensity for the GaAs(100) $c(4\times4)$ substrate with As_4 introduced during the MBE growth of Ge. This novel type of stationary cation analysis provides the clearest picture of the interface-growth process. Comparing Fig. 10 with Fig. 5, it is clear that the presence of As_4 during Ge-overlayer growth drastically alters the onset of the curve. However, while the initial monolayer formation is modified, in both cases the same amount of As segregates at the final free Ge surface. Similar behavior has been observed for the GaAs(100) 4×6 and $c(2\times8)$ surface reconstructions, as shown in the figure.

B. Electron affinity

Another parameter that is sensitive to the presence of As during interface formation is the electron affinity χ of the free surface. We have measured the changes in χ with respect to the initial value by subtracting the change in band bending from the change in work function with increasing Ge coverage. These quantities are determined experimentally by measuring the Ga(3d) energy position and the secondary electron-distribution cutoff, respectively.[27] Figure 11 shows the change in the electron affinity, $\Delta\chi$,

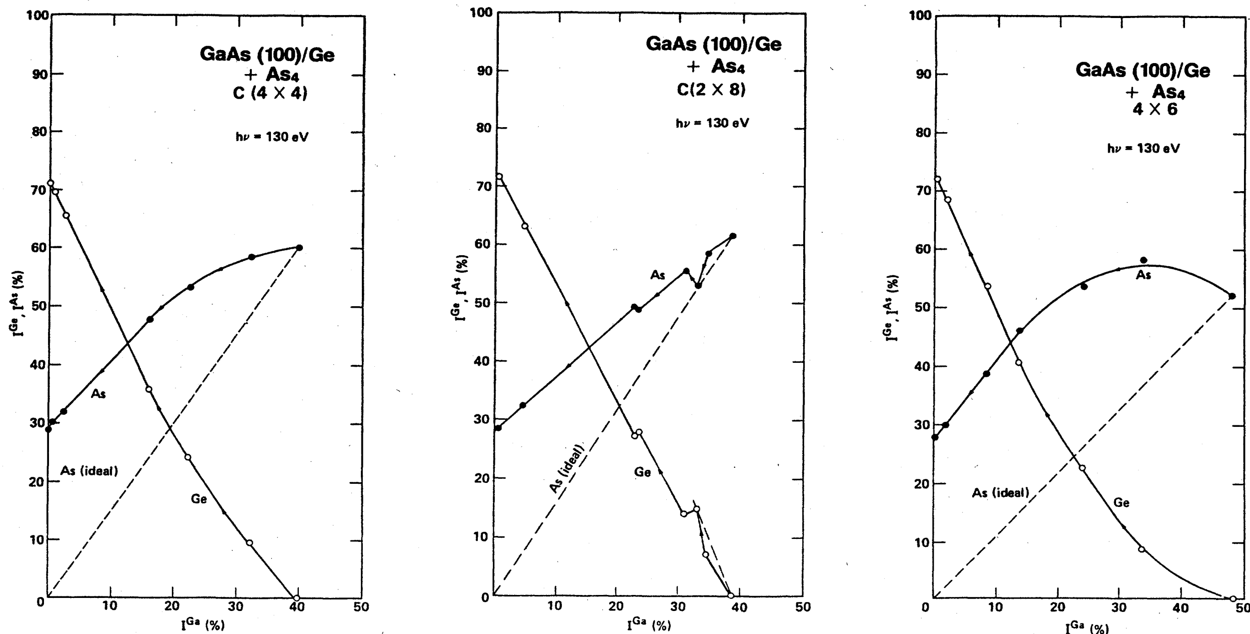

FIG. 10. Stationary cation analysis: As(3d) and Ge(3d) relative intensities are plotted vs the Ga(3d) relative intensity for the different starting surfaces of GaAs(100) and for consecutive coverages of Ge in the presence of an overpressure of As_4. The influence of As_4 is clear from the onset of the curves. However, the final amount of As is the same regardless of starting surface and the overpressure of As_4.

as a function of Ge coverage for three initial surface reconstructions, namely 4×6, $c(2\times8)$, and $c(4\times4)$. The electron affinity referenced to the substrate tends to increase upon heterojunction growth. This behavior can be explained by the dipole associated with the As—Ge bond at the interface. The decrease in χ shown in Fig. 11 for the $c(4\times4)$ surface is attributed to the dipole created by the first monolayer of Ge on top of the As-terminated surface. At a larger coverage an exchange reaction between Ge and As takes place and, therefore, the microscopic dipole *reverses* its orientation.

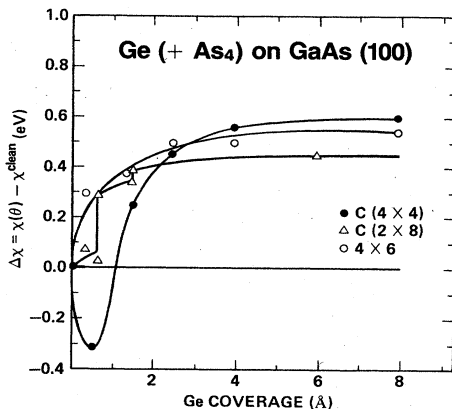

FIG. 11. Evolution of the electron affinity χ during interface formation between different starting surfaces of GaAs(100) and Ge. The Ge overlayer was deposited on the substrate at 320 °C in the presence of an overpressure of As_4. The zig-zag behavior observed for the $c(2\times8)$ surface is attributed to changes in χ due to exposing the surface to As_4 after depositing the Ge overlayer.

C. Fermi level

Finally, the Fermi-level position at the GaAs(100)/Ge interface correlates with the As/Ga ratio of the initially clean surface. The presence of As during overlayer growth serves only to emphasize this correlation. An excess of As in the interface region moves the Fermi level upward in the gaps until it reaches the top of the Ge conduction band. This effect can simply be explained in terms of As acting as an electron donor in Ge.[49,50] The principle of detailed balance requires a redistribution of the charges on both sides of the interface (i.e., transfer of charge from the Ge side to the GaAs side).

D. Band offsets

It is remarkable that, despite all these modifications induced by the presence of As_4 during interface growth, the band offsets are by no means affected by such a change in the environmental conditions. Figure 12 summarizes our experimental ΔE_v values for the different GaAs/Ge(100) interfaces with and without As_4 during the Ge-film growth. No differences or trends are detectable within an experimental uncertainty of ±0.05 eV. We interpret this result as being caused by strong local electrostatic forces during the initial stages of interface formation. Such forces prevent modification of the built-in potential barrier by introducing As "foreign" species. These measurements provide further support for theories that account for bulk properties of semiconductors being the most suitable for describing heterojunction band offsets.

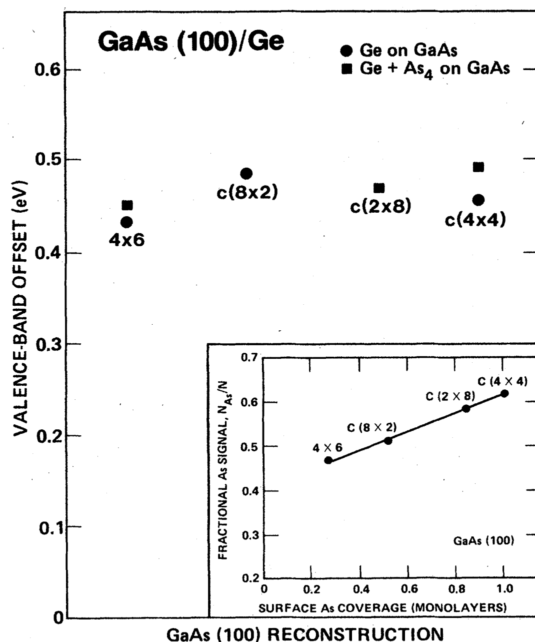

FIG. 12. Experimental values of the valence-band offset for GaAs/Ge(100) and various initial reconstructions. The measured values of the band offset for all the interfaces we studied here are within a band of ±0.05 eV. This suggests that the contribution of the local properties of the interface is not larger than ±0.05 eV. The inset shows the As/Ga ratio for various reconstructions of the GaAs(100) surface as obtained from our core-level photoemission studies.

VI. SUMMARY AND CONCLUSIONS

Our photoemission study shows that the As species is involved in a series of chemical processes at the interface and 1 ML of As is segregated at the surface of a thick Ge overlayer. In addition, it shows that if Ga does have any strong chemical activity, then it is confined to the interfacial region. This stationary position of the cation is used as a novel method for analyzing the evolution of the different atomic constituents during the heterojunction growth, independent of the Ge overlayer thickness. The band offsets for the abrupt GaAs/Ge(100) heterojunction is independent of the reconstruction and As/Ga ratio of the initial clean substrate to within the experimental uncertainty of ±0.05. The measured band offset is (0.47±0.05) eV. It is the same for all the interfaces we studied regardless of the surface reconstruction, the As/Ga ratio of the starting surface, the Fermi-level position in the gap, or the As_4 presence in the growth environment during interface formation. This experimental result would be accounted for in a simple way if we assume that the chemical composition and ordering of the interfacial region are the same independent of the initial GaAs substrate reconstruction and surface-As concentration. In any event the different kind of chemical and structural variations we induced at the intimate GaAs/Ge(100) interface do *not* contribute to ΔE_v by more than ±0.05 eV. Such a result explains the success of the purely bulk semiconductor model for heterojunction band offsets.[12,13] The observation of E_F changes throughout half the band gap, while that ΔE_v remains constant suggests that an internal chemical potential is not a useful concept to replace the incorrect surface electron affinity rule.[9] Rather, Harrison's linear combination of atomic orbitals model or a common anion rule is presently the most successful description of the experimental results.

ACKNOWLEDGMENTS

This work was partly funded by the Office of Naval Research (L. Cooper) under Contract Nos. N0001-81-C-0696 and N0001-84-C-0338. Further gratitude is extended to L. Cooper for his interest in our research, continuous support and, above all, for stimulating discussions. The experiments were conducted at SSRL, which is supported by the Department of Energy, Office of Basic Energy Sciences; National Science Foundation, Division of Materials Research; and the National Institute of Health, Biotechnology Resource Program, Division of Research Resources. We would like to thank H. Kroemer and T. McGill for very stimulating and productive discussions.

---

*Present address: Istituto Struttura Materia, via Enrico Fermi 38, Frascati, Roma 00044, Italy.

†Present address: Physics Department, University of Colorado, Boulder, CO 80309.

[1]A. G. Milnes and D. L. Feucht, *Heterojunctions and Metal-Semiconductor Junctions* (Academic, New York, 1972).

[2]P. Perfetti, N. G. Stoffel, A. D. Katnani, G. Margaritondo, C. Quaresima, F. Patelli, A. Savoia, C. M. Bertoni, C. Calandra, and F. Mandhi, Phys. Rev. B **24**, 6174 (1981).

[3]P. Perfetti, D. Denley, K. A. Mills, and D. A. Shirley, Appl. Phys. Lett. **33**, 66 (1978); D. Denley, K. A. Mills, P. Perfetti, and D. A. Shirley, J. Vac. Sci. Technol. **16**, 1501 (1979).

[4]R. S. Bauer and J. C. McMenamin, J. Vac. Sci. Technol. **15**, 1444 (1978).

[5]G. A. Baraff, J. A. Appelbaum, and D. R. Hamann, Phys. Rev. Lett. **38**, 237 (1977).

[6]Warren Pickett, Steven G. Louie, and Marvin Cohen, Phys. Rev. B **17**, 815 (1978).

[7]J. Pollman and S. Pantelides, J. Vac. Sci. Technol. **16**, 1498 (1979); C. A. Swart, W. A. Goddard, and T. C. McGill, *ibid.* **19**, 551 (1981).

[8]M. J. Adam and Allen Nussbaum, Solid-State Electron. **22**, 783 (1979); Oldwig Van Ross, *ibid.* **23**, 1069 (1980).

[9]R. L. Anderson, Solid-State Electron. **5**, 341 (1962).

[10]R. Dingle, in *Festkörperprobleme (Advances in Solid State Physics)*, edited by H. J. Queisser (Vieweg, Braunschweig, 1975), Vol. 15, p. 21.

[11]J. O. McCaldin, T. C. McGill, and C. A. Mead, Phys. Rev. Lett. **36**, 56 (1976).

[12]W. Harrison, J. Vac. Sci. Technol. **14**, 1016 (1977).

[13]W. R. Frensley and H. Kroemer, Phys. Rev. B **15**, 2642 (1977).

[14]R. S. Bauer, P. Zurcher, and H. W. Sang, Jr., Appl. Phys. Lett. **43**, 663 (1983).

[15]G. Margaritondo, A. D. Katnani, N. G. Stoffel, R. R. Daniels, and Te-Xiu Zhao, Solid State Commun. **43**, 163 (1982).

[16]A. D. Katnani, R. R. Daniels, Te-Xiu Zhao, and G. Margaritondo, J. Vac. Sci. Technol. **20**, 662 (1982); A. D. Katnani, N. G. Stoffel, R. R. Daniels, Te-Xiu Zhao, and G. Margaritondo, *ibid.* A **1**, 692 (1983).

[17]A. D. Katnani and G. Margaritondo, J. Appl. Phys. **5**, 2522 (1983) (references therein should give the reader many references to consult).

[18]A. D. Katnani and G. Margaritondo, Phys. Rev. B **28**, 1944 (1983).

[19]J. R. Waldrop and R. W. Gant, Phys. Rev. Lett. **26**, 1686 (1978).

[20]E. A. Kraut, R. W. Gant, J. R. Waldrop, and S. P. Kowalczyk, Phys. Rev. Lett. **44**, 1620 (1980).

[21]S. P. Kowalczyk, E. A. Kraut, J. R. Waldrop, and R. W. Gant, J. Vac. Sci. Technol. **21**, 482 (1982); S. P. Kowalczyk, W. J. Schlaffer, E. A. Kraut, and R. W. Gant, *ibid.* **20**, 705 (1981).

[22]R. W. Gant, J. R. Waldrop, and E. A. Kraut, Phys. Rev. Lett. **40**, 656 (1978).

[23]W. Monch and R. W. Gant, J. Vac. Sci. Technol. **17**, 1094 (1980).

[24]W. Monch, R. S. Bauer, H. Gant, and R. Marschal, J. Vac. Sci. Technol. **21**, 498 (1982).

[25]W. Monch and R. W. Gant, Phys. Rev. Lett. **48**, 512 (1982).

[26]R. S. Bauer and J. C. Mikkelsen, J. Vac. Sci. Technol. **21**, 491 (1982).

[27]P. Zurcher and R. S. Bauer, J. Vac. Sci. Technol. A **1**, 695 (1983).

[28]R. S. Bauer and H. W. Sang, Jr., Surf. Sci. **132**, 479 (1983).

[29]R. S. Bauer, Thin Solid Films **89**, 419 (1982), and references therein.

[30]R. Z. Bachrach, R. S. Bauer, P. Chariadia, and G. V. Hansson, J. Vac. Sci. Technol. **18**, 797 (1981); **19**, 335 (1981).

[31]P. K. Larsen and J. F. van der Veen, Surf. Sci. **126**, 1 (1983).

[32]J. H. Neave, P. K. Larsen, B. A. Joyce, J. P. Gowers, and J. F. van der Veen, J. Vac. Sci. Technol. B **1**, 668 (1983).

[33]P. K. Larsen, J. H. Neave, J. F. van der Veen, P. J. Dobson, and B. A. Joyce, Phys. Rev. B **27**, 4966 (1983); J. F. van der Veen, P. K. Larsen, J. H. Neave, and B. A. Joyce, Solid State Commun. **49**, 659 (1984), and references therein.

[34]J. Massies, P. Devoldere, and N. T. Linb, J. Vac. Sci. Technol. **16**, 1244 (1979).

[35]R. S. Bauer and T. C. McGill, in *VLSI Electronics: Microstructure Science,* edited by N. G. Einspruch (Academic, New York, 1985), Vol. 10, p. 3; A. Zur and T. C. McGill, J. Vac. Sci. Technol. B **2**, 440 (1984).

[36]A. D. Katnani, P. Chariadia, H. W. Sang, Jr., and R. S. Bauer, J. Vac. Sci. Technol. (to be published).

[37]A. D. Katnani, H. W. Sang, Jr., P. Chariadia, and R. S. Bauer, J. Vac. Sci. Technol. B**2**, 471 (1984).

[38]Y. Mizokawa, H. Iwasak, R. Nishitani, and S. Nakamura, J. Electron Spectrosc. Relat. Phenom. **14**, 129 (1978).

[39]F. Stucki, G. J. Lapeyre, R. S. Bauer, P. Zurcher, and J. C. Mikkelsen, J. Vac. Sci. Technol. **1**, 865 (1983).

[40]E. A. Kraut, R. W. Gant, J. R. Waldrop, and S. P. Kowalczyk, Phys. Rev. B **28**, 1965 (1984).

[41]W. E. Spicer, P. W. Chye, P. R. Skeath, C. Y. Su, and I. Lindau, J. Vac. Sci. Technol. **16**, 1428 (1979); W. E. Spicer, I. Lindau, P. R. Skeath, and C. Y. Su, *ibid.* **17**, 1019 (1980); W. E. Spicer, I. Lindau, P. R. Skeath, C. Y. Su, and P. W. Chye, Phys. Rev. Lett. **44**, 420 (1980).

[42]L. J. Brillson, Surf. Sci. Rep. **2**, 123 (1982).

[43]I. Lindau and W. E. Spicer, J. Electron Spectrosc. Relat. Phenom. **3**, 409 (1974).

[44]L. J. Brillson, R. S. Bauer, R. Z. Bachrach, and G. V. Hansson, Phys. Rev. B **23**, 6204 (1981).

[45]G. Margaritondo, Solid-State Electron. **26**, 499 (1983).

[46]B. Mrstik, Surf. Sci. **124**, 253 (1982).

[47]J. E. Northrup (private communication).

[48]Marvin L. Cohen, in *Advances in Electronics and Electron Physics,* edited by L. Marton and C. Marton (Academic, New York, 1980), Vol. 51, p. 1.

[49]P. Chariadia, A. D. Katnani, H. W. Sang, Jr., and R. S. Bauer, Phys. Rev. Lett. **52**, 1246 (1984).

[50]A. D. Katnani, P. Chariadia, H. W. Sang, Jr., and R. S. Bauer (unpublished).

[51]E. A. Kraut, J. Vac. Sci. Technol. B **1**, 643 (1983).

[52]W. A. Harrison, E. A. Kraut, J. R. Waldrop, and R. W. Gant, Phys. Rev. **18**, 4402 (1978).

[53]B. A. Joyce and C. T. Foxon, J. Cryst. Growth **31**, 122 (1975).